Catalysis Today 154 (2010) 105–112

Contents lists available at ScienceDirect

Catalysis Today

journal homepage: www.elsevier.com/locate/cattod

Unsolved problems in catalysis

Ken-ichi Tanaka

Saitama Institute of Technology, Research Center of Advanced Sciences, 1690 Okabe, Fukaya, Saitama, Japan

ARTICLE INFO

Article history:
Available online 13 April 2010

Keywords:
Activation of catalyst
Intermediates
Turn over frequency
Role of promoter
Surface restructuring
NO_x reduction
Olefin metathesis
PROX reaction of CO
Isomerization and hydrogenation of olefins

ABSTRACT

It is not so difficult to detect adsorbed atoms and molecules on solid surfaces, but their reaction processes are still difficult to direct. Catalysis is caused by the ensemble operation of their reaction via intermediates on active sites, and suitable elementary reactions are supposed to explain the catalysis. Accordingly, unsettled problems in catalysis are caused by our lack of knowledge about the dynamics of elementary processes. In this paper, activity of the catalyst is discussed from the following points; (i) activation by restructuring, (ii) activation by forming active sites and reactive intermediates, (iii) site dependent turnover frequency, and (iv) role of promoting materials.

1. Introduction—what we know and what we do not know

Before 1960, catalysis was explained by reaction kinetics, because we had no tools to inspect the catalyst surface. At the present time, we can inspect not only the lattice atoms but also adsorbed atoms and molecules on the surface. However, it is still difficult to detect the reacting process itself, which involves transport of atoms and molecules and intermediates to active sites and exthothermic and endothermic elementary reactions. Therefore, catalysis taking place on the surface is explained by assuming suitable elementary reactions. In 1921, Langmuir [1] observed roughening of catalyst surface and postulated catalysis on sites with suitable lattice distances. About 40 years later of 1964, Germer [2] wrote in his review "the most significant result that has been obtained up to this time from LEED studies is the observation of "reconstruction".

However, it was still difficult to get reliable data of the adsorption of simple molecules on clean and well-defined surfaces in 1960, and thermo-dynamical data were obtained by using evaporated metal films, as summarized by Bond [3] in his book. Accumulation of the data, however, helped us to consider how the reaction was promoted on metal surfaces. For example, Sachtler and Reijen [4] showed a volcano-shaped relationship between the activity of metals in the decomposition of HCOOH and the stability of metal formate, which was compatible to Sabatier's empirical prediction, and Tanaka and Tamaru [5] showed a general tendency of metals in the adsorption of various molecules. On the other hand, an idea of active sites proposed by Taylor [6] for adsorption of molecules has been accepted as the catalysis by specific sites. For example, Thomson and Wishlade [7] demonstrated, using radioactive ethylene–C^{14}, that a limited part of a Ni-film was active for the hydrogenation of ethylene. In this circumstance, Tamaru [8] showed the importance of studying the real intermediates and their dynamics during catalysis, because observed adsorbed species are not always the reaction intermediates.

In the early 1970s, Somorjai and coworkers [9,10] challenged the pioneering works on catalysis using well-defined single-crystal surfaces. A typical result was the structure-dependent activity of single-crystal Fe surfaces in ammonia synthesis reaction, Fe(1 1 1) ≫ Fe(1 0 0) ≫ Fe(1 1 0). He also showed notable promoting effect of Al_2O_3 on the activity of Fe surfaces in ammonia synthesis reaction. By the deposition of 2-monolayers of Al_2O_3 and subsequent treating in H_2O at 723 K, the Fe(1 0 0) and (1 1 0) surfaces change to highly active surfaces being almost equal to that of the Fe(1 1 1) surface [11]. The reaction mechanism of ammonia synthesis as well as ammonia decomposition has been widely studied on various metals, and it is deduced that the dissociation of N_2 (desorption of N_2 in the decomposition reaction of NH_3) is the rate-determining step of ammonia synthesis reaction on various metals. Accordingly, we could say that activity in the dissociation of N_2 is responsible for the activity in the ammonia synthesis reaction. If this is the case, the dissociation rate of N_2 (or the recombination rate of N atoms) on Fe surfaces should be enhanced in the presence of Al_2O_3, but the mechanism of enhancement is still unsettled. The role of Al_2O_3 in ammonia synthesis reaction is undoubtedly an interesting subject in the area of promoting materials.

E-mail address: ktanaka@sit.ac.jp.

0920-5861/$ – see front matter © 2010 Elsevier B.V. All rights reserved.
doi:10.1016/j.cattod.2010.03.015

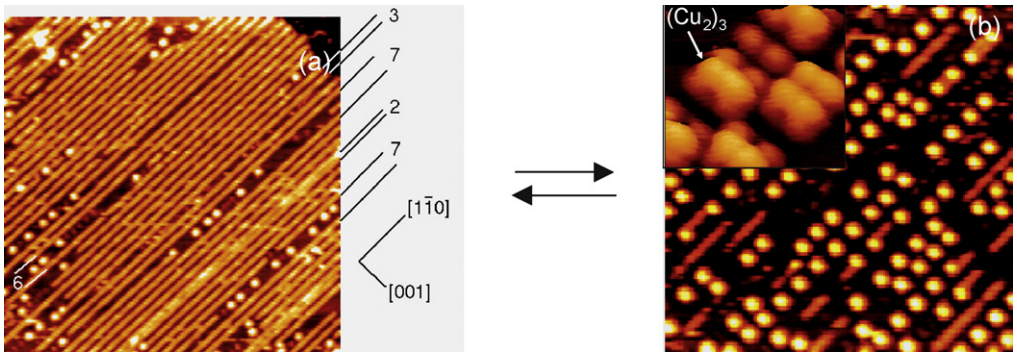

Fig. 1. (a) (–Cu–O–) Chain prepared on an Ag(1 1 0) surface and its decomposition into $(Cu_2)_3$ dots along the phase boundary of a (3×1) array (526 A × 526 A). (b) Growing of a (–Cu–O–) chain by exposing a $(Cu_2)_3$/Ag(1 1 0) surface to O_2 at room temperature (260 A × 260 A). Inset image shows the array of Cu atoms in a $(Cu_2)_3$ cluster (37 A × 37 A).

In 1983, a landmark paper was published by Binnig et al. [12], which demonstrated the potential of scanning tunneling microscopy (STM) to inspect the solid surfaces at atomic resolution. In 1987, Ertl and coworkers [13] applied an STM to the adsorption of oxygen on a Cu(1 1 0) surface, and showed the reconstruction of the Cu(1 1 0) surface in the real space. In 1991, Tanaka and coworkers [14] shed light on the mechanism of continuous structure change of the Ag(1 1 0) surface from $p(7 \times 1)$ to $p(2 \times 1)$ with increasing oxygen coverage. In the same year, Nielsen et al. [15] demonstrated that formation of a (1×2) Ni(1 1 0)-H surface in H_2 at room temperature was different from the (1×2) Ni(1 1 0) surface induced by pairing of Ni rows below 220 K. They also reported compression of the array of (–Ni–O–) from (3×1) to (2×1) by growing (–Ni–H–) strings in H_2 [16]. Tanaka [17,18] explained these real space restructuring processes by a new concept of "quasi-compound", which is stabilized by a periodic interaction with a surface. According to this concept, formation of a quasi-compound of (–Cu–O–) strings on Ag(1 1 0) surface was demonstratively shown [19,20]. Reversible formation and decomposition of the quasi-compound of (–Cu–O–) strings on an Ag(1 1 0) surface are shown in Fig. 1(a) and (b), where (–Cu–O–) strings arrayed with a (1×3) periodicity on an Ag(1 1 0) surface undergo decomposition along the phase boundary of the (1×3) structure at ca. 500 K and square $(Cu_2)_3$ clusters are formed. An inset image in Fig. 1(b) shows the atomic structure of $(Cu_2)_3$ cluster and a Cu_2 left from formation of $(Cu_2)_3$ clusters.

It is a notable fact that the formation and the decomposition of quasi-compound of (–Cu–O–) is a reversible reaction on the Ag(1 1 0) surface, that is, the $(Cu_2)_3$ cluster on Ag(1 1 0) reacts with O_2, $(Cu_2)_3 + O_2 \rightarrow$ (–Cu–O–), at room temperature, as shown in Fig. 1(b). If $(Cu_2)_3$ could react with NO to form (–Cu–O–) and N_2, a thermodynamic probable direct decomposition of NO into N_2 and O_2 would be catalyzed, but no such system has been found.

Somorjai expressed the dramatic change of the catalytic activity by restructuring and/or modification by an idea of "flexible surface", but the mechanism of improvement is still not clear. In this respect, even if one can inspect the surface at atomic resolution, the improvement of catalysis is one of the unsettled problems as discussed in this paper.

2. Activation of catalyst

A catalytic reaction is comprised of several elementary processes, and the reaction rate and the rate equation (kinetics) depend on the rat-determining step. Here, I will explain how the activity of catalyst be changed by (pre-) treatment.

2.1. Activation by restructuring

When metals are exposed to reactive molecules, most metal surfaces are restructured by the adsorption or the reaction of molecules. Accordingly, the catalysis by metals cannot be simply explained by the original structure and properties of the clean surface.

Here I take up an example of the Pt–Rh alloy surface. Pt–Rh alloy or bimetal is known as three-way catalyst with high performance to lower the NO_x, CO, and hydrocarbons in automotive exhaust. The Pt/Rh ratio of the surface is widely changed by the adsorption, chemical reaction, and temperature. Nieuwenhuis and coworkers [21] studied precisely the labile property of a $Pt_{0.25}Rh_{0.75}$(1 0 0) surface by measuring surface fraction of Pt and Rh atoms. As shown in Fig. 2(a), the Pt–Rh(1 0 0) surface reaches equilibrium at temperatures above ~1000 K (about a half of the melting temperature of Pt (1997 K) and Rh (2249 K)), but the Pt fraction is higher on the surface compared to that of the bulk below 1400 K. That is, the equilibrium composition of the $Pt_{0.25}Rh_{0.75}$(1 0 0) surface becomes almost equal to that of the bulk fraction at temperature above 1400 K. However, it was not clear how such surface composition influences the catalysis. As shown in Fig. 2(a), the Pt/Rh ratio changes very slowly in vacuum below 1000 K, but notably the Pt/Rh ratio changes very rapidly in NO or O_2 even at 400 K and gives a characteristic $p(3 \times 1)$ LEED pattern as shown in Fig. 2(b) [22]. The $p(3 \times 1)$ $Pt_{0.25}Rh_{0.75}$(1 0 0)–O surface is formed by replacement of the Rh atoms in the 2nd layer with the Pt atoms in the topmost layer in NO or O_2. The formation of same $p(3 \times 1)$ structure was confirmed by heating a Pt deposited Rh(1 0 0) surface [23,24] and a Rh deposited Pt(1 0 0) surface [25,26] in O_2, where Pt or Rh was deposited in an electrochemical cell grafted to the UHV chamber. Fig. 2(c) shows a STM image of the $p(3 \times 1)$ $Pt_{0.25}Rh_{0.75}$(1 0 0) surface first observed by Tanaka and his coworkers [27], where the Pt and Rh atoms were distinguishable on the $p(3 \times 1)$ Pt–Rh(1 0 0)–O surface by changing the bias potential. An interesting fact is that the surface becomes active for the reduction of NO with H_2, $NO + H_2 \rightarrow N_2 + H_2O$ by surface restructuring forming a $p(3 \times 1)$ structure as shown in Fig. 2(d) [23,26]. This result suggests that a specific array of Pt and Rh atoms may give high catalytic activity for the reduction of NO with H_2. It was also shown that Pt/Rh(1 0 0), Rh/Pt(1 0 0), Pt/Rh(1 1 0), and Rh/Pt(1 1 0) bimetal surfaces became active by restructuring for the reduction of NO with H_2 [28]. Therefore, we deduced that some specific array of the Pt and Rh atoms induced by the adsorption of oxygen may be active for the reduction of NO, but it is unsettled how the specific array of Pt and Rh atoms enhances rate-determining step of NO reduction.

2.2. Activation by forming active sites and reactive intermediates

In the preceding section, we discussed the activation caused by surface restructuring. In this section, we focus on the activation by forming active sites or by providing reactive precursor molecules during catalysis.

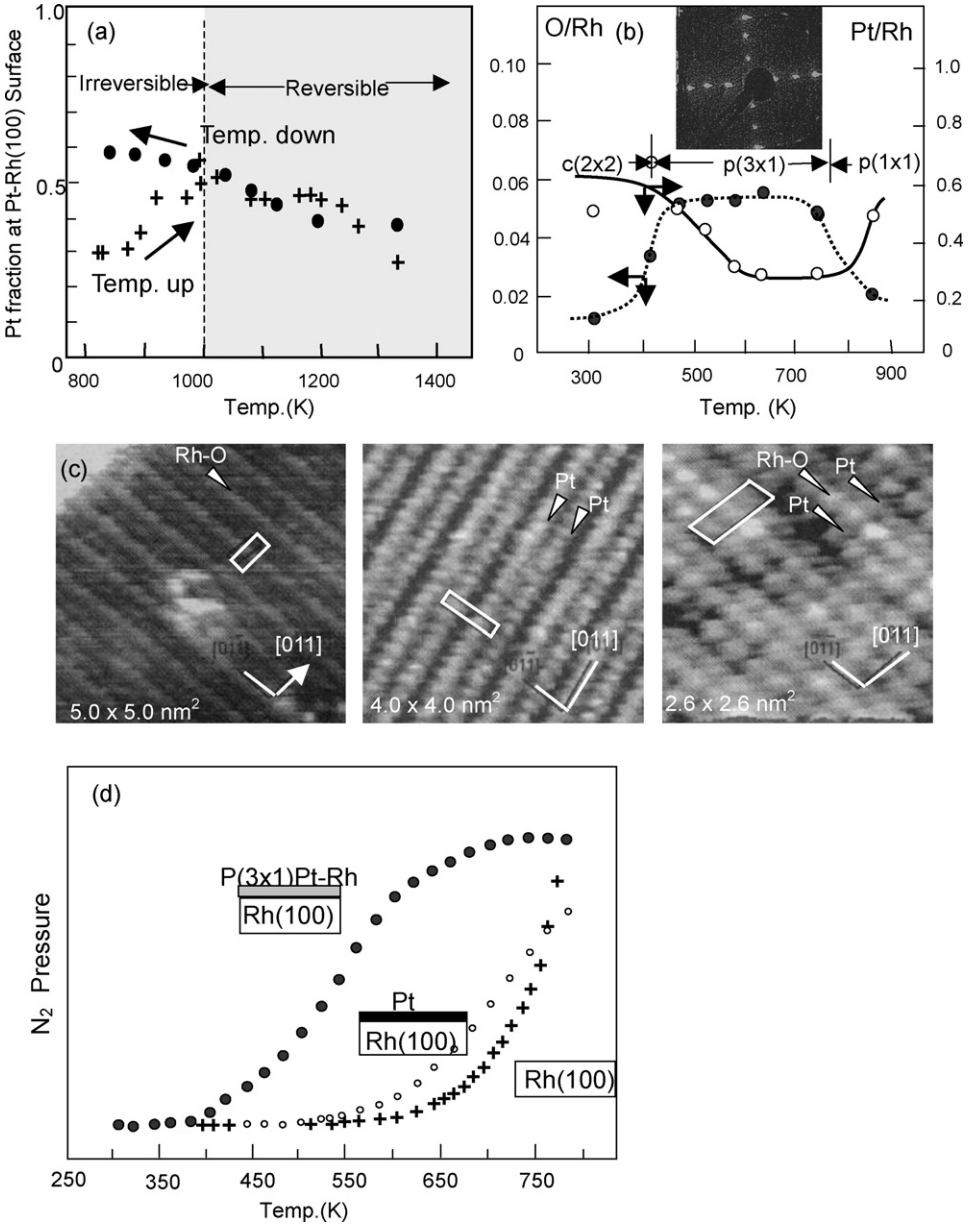

Fig. 2. (a) Reversible change of Pt fraction of $Pt_{0.25}Rh_{0.75}(1\,0\,0)$ surface by raising and lowering temperature in vacuum. (b) Changing of the $Pt_{0.25}Rh_{0.75}(1\,0\,0)$ surface heated in 10^{-7} Torr of O_2 for 5 min at various temperatures. The surface showing a $p(3\times1)$ LEED pattern has the constant ratio of O/Rh and Pt/Rh. (c) The STM images of a $p(3\times1)$ $Pt_{0.25}Rh_{0.75}(1\,0\,0)$–O surface. The Pt, Rh and (–Rh–O–) were distinctive at different bias potentials. (d) $p(3\times1)$ Pt deposited Rh(1 0 0) surface is active for catalytic reduction of NO with H_2.

Catalysis sometimes is caused by the formation of reactive molecules or compounds which is an additional new reaction path. One example is the reduction of NO_x with C_3H_6 on Ag/Al_2O_3 catalyst enhanced by H_2 [29–33]. The activation was explained by a structural change of the catalyst by H_2 by Shibata et al. [31], but Breen et al. [32] presumed the formation of reactive C=N species during catalysis. On the other hand, He and coworkers [34,35] proposed a new reaction path via enolic species (RCH=CH–O–). That is, enolic species are formed by partial oxidation of C_2H_5OH or C_3H_6 and they react with NO_x to form reactive Ag–NCO, and finally, NCO reacts with NO to form N_2 and CO_2. In this mechanism, providing enolic species (RCH=CH–O–) on Ag/Al_2O_3 is essential in the catalytic oxidation of hydrocarbon with O_2. Interestingly, it was also shown that enolic species play an important role in burning flame [36]. Nakajima and coworkers found that complete reduction of NO_x with NH_3 on Fe_2O_3–TiO_2 catalyst requires a certain amount of O_2 as shown in Fig. 3 [37]. In this case, the NO/NO_2 ratio is adjusted to 1/1 by O_2, which is the role of O_2 enhancing the reduction of NO_x, but the reaction mechanism with NH_3 taking place at $NO/NO_2 = 1$ is not clear.

It is known that some chemical reactions are promoted by some molecules other than reactants, the enhancement of catalysis by other than reactants might be similar phenomenon. From this view point, catalytic reduction of WO_3 by H_2 in the presence of Pt/Al_2O_3 is an interesting example. As shown by Levy and Boudart [38], yellow WO_3 reduces very slowly to blue $H_xWO_{3-x/2}$ in dry H_2 at 50 °C in the presence of Pt/Al_2O_3 catalyst, but changes to blue color very rapidly at room temperature when H_2O or alcohol is contained in H_2. In this case, the mechanism was explained by H_2O assisted ionization of H_2 molecule forming H_3O^+ on Pt and its transportation onto WO_3, where the H_3O^+ reacts on WO_3 with electron transported through the bulk to form blue $H_xWO_{3-x/2}$. This mechanism

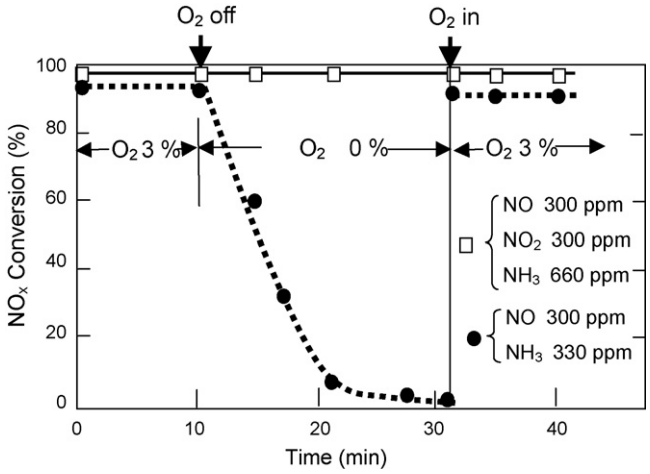

Fig. 3. Complete removal of NO_x by NH_3 required a certain amount of O_2 on the Fe_2O_3–TiO_2 catalyst at 350 °C. SV = 30,000 h^{-1}.

is analogous to formation of H_3O^+ in the presence of H_2O on the Pt-anode of a hydrogen fuel cell, and its transportation through a polymer electrolyte film onto the cathode.

Another important activation is a self-activation of catalyst by reactant molecules. In this case, it is difficult to recognize the activation the presence of a detectable induction time. Catalysis on a layer compound of MoS_2 is a good example. The basal plane of MoS_2 is completely covered with a sulfur layer and catalysis is caused by the flank of MoS_2 crystal. Fig. 4(a) shows the activation of single-crystal MoS_2 flakes, where the flank surface becomes active for the isomerization of but-1-ene with an induction time by adding H_2. The activation the flank surface is explained by the formation of Mo–H and H–Mo–H sites in H_2. When H_2 was added to but-1-ene on ordinary fine powder of MoS_2, the isomerization reaction as well as the hydrogenation of but-1-ene occurs with no induction time as shown in Fig. 4(b).

Such simultaneous isomerization and hydrogenation of olefins was explained by a mechanism of so-called the Horiuti–Polanyi type, presuming a common alkyl intermediate for the hydrogenation and the isomerization of olefins. That is, the isomerization is explained by a reverse reaction from an alkyl intermediate for the hydrogenation reaction. However, addition of D_2 (deuterium) to but-1-ene on the MoS_2 catalyst yielded but-2-ene-$[^2H]_0$ in more than 90% ($[^2H]$ denotes the D atom) but the hydrogenation reaction yielded butane-1,2-$[^2H]_2$ in more than 80%, as shown in Fig. 4(b). This result is evidently disagreement with the Horiuti–Polanyi mechanism, that is, the sec-butyl for the isomerization is not the intermediate for the hydrogenation of but-1-ene. We can conclude that the two reactions proceed via alkyl intermediates but occur on different active sites [39,40].

Different coordinative unsaturation of the Mo atoms on the flank surfaces of MoS_2 is responsible for the formation of different functional sites by exposing to H_2. Formation of different functional sites on MoS_2 was also proved by the isotope scrambling in a mixture of C_2H_4/C_2D_4 (3/2) + H_2/D_2 (2/3), that is, the isotope scrambling in $C_2H_4 + C_2D_4 \leftrightarrow C_2H_3D + C_2D_3H$ and that in $H_2 + D_2 \leftrightarrow 2HD$ proceed independently [40,41]. Existence of different functional sites is also essential to consider the scientific meaning of the turnover frequency per site as will be discussed in the next section.

2.3. Site dependent turnover frequency

Turnover frequency (TF) is defined as the activity per site. However, real reaction may not occur as assumed in the definition. That is, TF may depend on the size of particles and on local configuration of active sites. In fact, the TF for an olefin metathesis reaction markedly depends on the configuration of active sites as shown in this section.

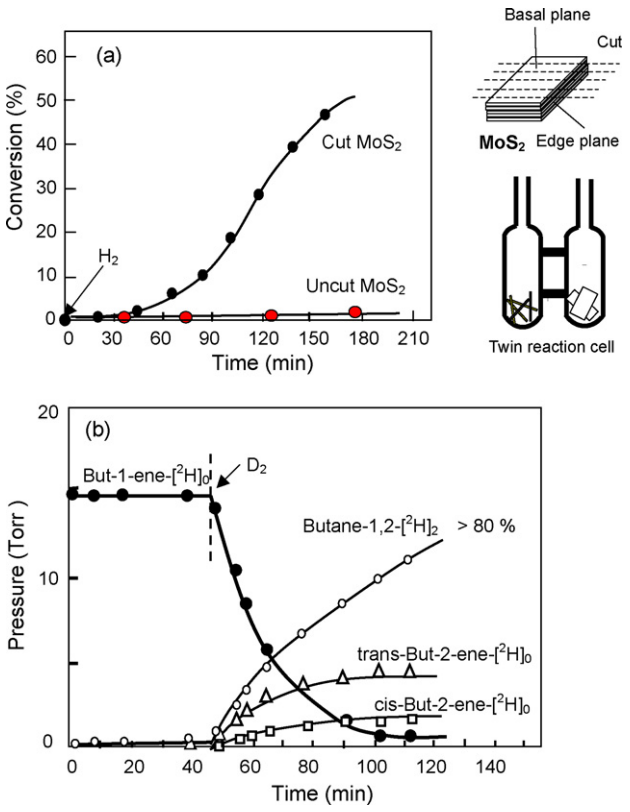

Fig. 4. (a) The flank surface of MoS_2 becomes active by adding H_2 for the isomerization reaction of but-1-ene with an induction time. The experiment was performed on two MoS_2 catalysts of which basal plane areas was nearly equal but flank surface areas was markedly different. (b) Hydrogenation and isomerization of but-1-ene was simultaneously enhanced by adding D_2. Hydrogenation yielded butane-1,2-$[^2H]_2$ in more than 80%, but the isomerization reaction taking place simultaneously yielded but-2-ene with no deuterium $[^2H]$ atoms.

MoO_3 film sublimated on a quartz wall of reactor had no activity for any reactions such as hydrogen exchange, isomerization, hydrogenation, and metathesis of olefins. However, if an olefin is condensed on this inactive MoO_3 film at liquid nitrogen and then treated with H atoms, the surface changes to a superior active catalyst for olefin metathesis reaction but no other reactions occur [43]. Similarly, if $Sn(CH_3)_4$ is adsorbed on the inactive MoO_3 film at room temperature, the MoO_3 film changes to a superior active catalyst for the olefin metathesis reaction as shown in Fig. 5 [42,43]. As no hydrogen scrambling occurs during metathesis reaction of olefins on this activated MoO_3 catalyst, productive metathesis (r_1) and degenerate metathesis (r_2) of propene can be measured by using a mixture of propene–$[^2H]_6$ and propene–$[^2H]_0$ according to Eq. (1). The result showed that the two metathesis reactions occurred by a ratio of $(r_2)/(r_1) = 10$–27. That is, degenerate metathesis (r_2) is one order of magnitude faster than productive metathesis (r_1). Why the TF differs more than 10 times between the degenerate and the productive metathesis of propene?

$$CD_2{=}CD{-}CD_3 + CH_2{=}CH{-}CH_3 \rightarrow \begin{cases} CH_2{=}CD_2 + CH_3{-}CH{=}CD{-}CD_3 & (r_1) \\ CD_2{=}CH{-}CH_3 + CH_2{=}CD{-}CD_3 & (r_2) \end{cases} \quad (1)$$

It has been established that olefin metathesis reaction proceeds via metalla-cyclobutane intermediates in homogeneous catalysis. If the olefin metathesis on this MoO_3 catalyst proceeds also via

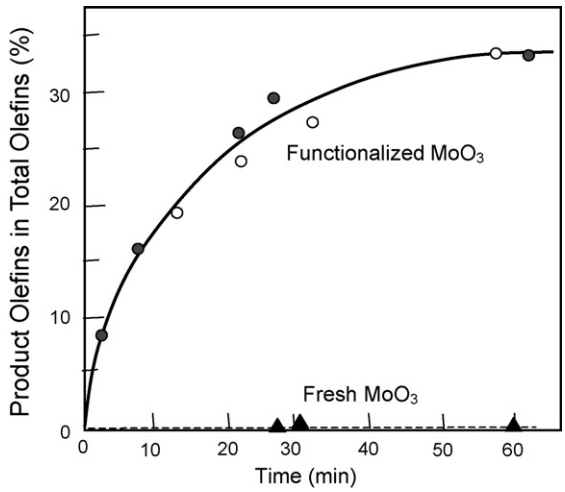

Fig. 5. Metathesis reaction of propene at room temperature on a MoO_3 film and a MoO_3 functionalized by reacting ethylene (●) or roppene (○) adsorbed at liq. N_2 temperature with H atom.

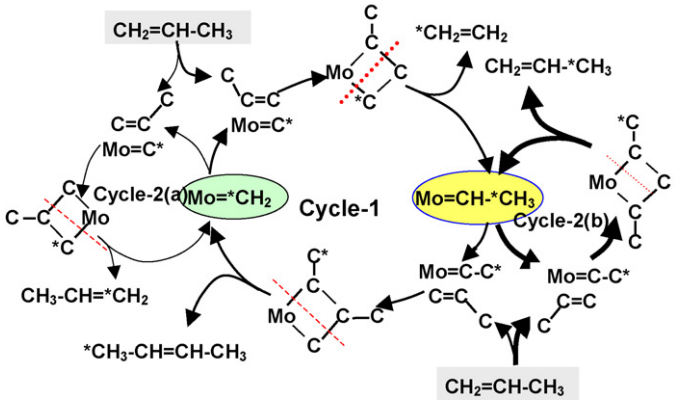

Scheme 1. An over-all mechanism of propene metathesis reactions via metallacyclo butane intermediates. Relative TF for the metathesis reaction is cycle-1/cycle-2(a)/cycle-2(b) = 1/10–30/100–900.

metalla-cyclobutane intermediates, an over-all mechanism of the metathesis reaction of propene is described in Scheme 1, where the reaction (r_1) in Eq. (1) is given by cycle-1 and the reaction (r_2) is given by cycle-2(a) and cycle-2(b). In this reaction scheme, alternative reaction of propene with Mo=CH_2 and Mo=$CHCH_3$ sites in cycle-1 gives the productive metathesis, and the reaction in cycle-2(a) and cycle-2(b) gives the degenerate metathesis. Orientation of propene molecule in a precursor state, either **(I)** or **(II)** in Scheme 2, decides the reaction going on the productive reaction (r_1) or the degenerate reaction (r_2). The value of r_1/r_2 = 10–27 proves that propene molecule prefers to take an orientation **(II)** on either the Mo=CH_2 or the Mo=$CHCH_3$ site.

Another interesting problem is the relative contributions of cycle-2(a) and cycle-2(b) in Scheme 1 in the degenerate metathesis of propene. This task was solved by performing the metathesis reaction between Z-propene-1-$[^2H]_1$ and CD_2=$CDCD_3$. If the degenerate metathesis of propene proceeds via metalla-

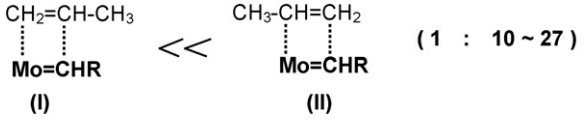

Scheme 2.

cyclobutane with two substituted methyl groups as in cycle-2(b), a daughter molecule would keep the Z-conformation of D to CH_3 of the parent Z-propene-1-$[^2H]_1$ molecule, and E-propene-1-$[^1H]_1$ is formed as described by Scheme 3 [44].

The result showed that the E-propene-1-$[^1H]_1$ was ca. 80% in Scheme 3. Therefore, the degenerate metathesis is predominantly catalyzed by Mo=$CHCH_3$ sites, that is, the degenerate metathesis occurs predominantly by cycle-2(b). Taking these results into account, the relative contribution was deduced to be cycle-2(a)/cycle-1/cycle-2(b) = 1/(10–30/)/(100–900) in the total metathesis reaction of propene. This is the first result showing real meaning of the TF per site. In other words, the scientific meaning of the traditional TF is not self-evident, that is, it is not necessarily correct to take a constant TF per site on particles when the size, morphology, and/or construction are different.

2.4. Role of promoting materials

It is well known that a small amount of additives can markedly change the activity and/or the selectivity of catalysts. In contrast, it is also known that the activity is influenced by supporting materials and in some cases improved by adding a large amount of promoting materials. In this section, the discussion is focused on large amounts of additives being indispensable in catalysis.

Effect of Al_2O_3 on ammonia synthesis reaction catalyzed by Fe surfaces [10] is a symbolic phenomenon of promotion by a large amount of additives. Well-defined Fe crystal surfaces have an activity sequence of Fe(1 1 1) ≫ Fe(1 0 0) ≫ Fe(1 1 0) for ammonia synthesis reaction, but the Fe(1 1 1), Fe(1 0 0), and Fe(1 1 0) surfaces covered with 2-monolayers of Al_2O_3 gave almost equally high catalytic activity for ammonia synthesis if these surfaces are treated in H_2O at 723 K. There is a long history of the ammonia synthesis reaction, and the reaction mechanism has been widely studied on various metals. It is now accepted that the dissociation of N_2 in a sequential mechanism of $1/2\,N_2 \rightarrow N \rightarrow NH \rightarrow NH_2 \rightarrow NH_3$ is the rate-determining step, and that the recombinative desorption step of N_2 is the rate-determining in the reverse ammonia decomposition reaction. Therefore, we expect that the dissociation of N_2 on Fe surface is improved by Al_2O_3, and the desorption (recombination) of N_2 from Fe surface is also enhanced by Al_2O_3. About the desorption of N_2, an interesting phenomenon was observed on a Pd(1 1 0) surface, that is, the special distribution of N_2 depends on the formation mechanism of N_2; $N(a) + N(a) \rightarrow N_2$, $NO + N(a) \rightarrow N_2 + O(a)$, and catalytic reaction of $NO + H_2 \rightarrow 1/2\,N_2 + H_2O$ on a Pd(1 1 0) gave different special distributions of N_2 [45–48]. In this respect, the effect of Al_2O_3 on the spatial distribution and the kinetic energy of N_2 desorbing from Fe surface is quite interesting.

Another example is the activation of a Pt(1 1 1) surface for the oxidation of CO by CeO_2 layers reported by Lambert and his coworkers [49]. They showed that the adsorption of CO on a Pt(1 1 1) surface decreased with increasing amount of CeO_2 deposited on the surface and no adsorption of CO occurred when the Pt(1 1 1) surface was covered with about 1.5 monolayers of CeO_2, and the activity for the oxidation of CO was markedly suppressed with increasing amounts of deposed CeO_2. However, the catalytic activity was suddenly improved when the deposition of CeO_2 on the Pt(1 1 1) surface was more than two monolayers. This phenomenon cannot be explained by the reaction taking place on Pt(1 1 1) surface, but the mechanism is still unsettled.

Recently, we found the oxidation of CO in H_2 on a Pt/TiO_2 catalyst was markedly improved by loading the Pt/TiO_2 with a large amount of FeOx [50,51]. Fig. 6(a) shows a typical result of the oxidation of CO in a flow of a mixture of CO (3.0 ml/min) + O_2 (1.5 ml/min) + H_2 (20 ml/min) + N_2 (75.5 ml/min). As it will be discussed below, low temperature oxidation of CO is explained by a new oxidation path via new intermediates in the presence of H_2 or H_2O. It should be

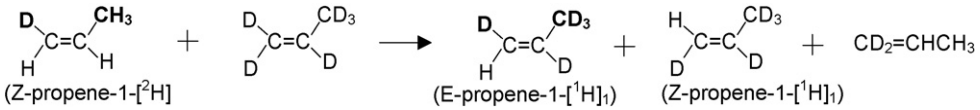

Scheme 3.

emphasized that the 1 wt.%Pt–TiO_2 (0.8 g) had rather low activity for the oxidation of CO at room temperature as shown in Fig. 6(a), but a FeO_x/Pt–TiO_2 (0.8 g) (ca. 140 wt.% by calculation as Fe_3O_4) was extremely active for the oxidation of CO at room temperature although the Pt in the FeO_x/Pt–TiO_2 was ca. 0.4 wt.%. Interestingly, poorly active Au/TiO_2 with large size of Au particles changed to an extremely active catalyst by loading FeOx [52]. This activation is entirely different from the size dependent activity reported by Haruta [53], which was explained by presuming the catalysis takes place at the perimeter of the Au particles. The role of FeOx could not be explained by this mechanism. Chen and Goodman [54] showed a specific activity of a (1×3) bi-layer structure Au atoms arrayed on a monolayer of titanium oxide, and they concluded that particle size of Au does not directly influence on the activity of Au/TiO_2 catalyst.

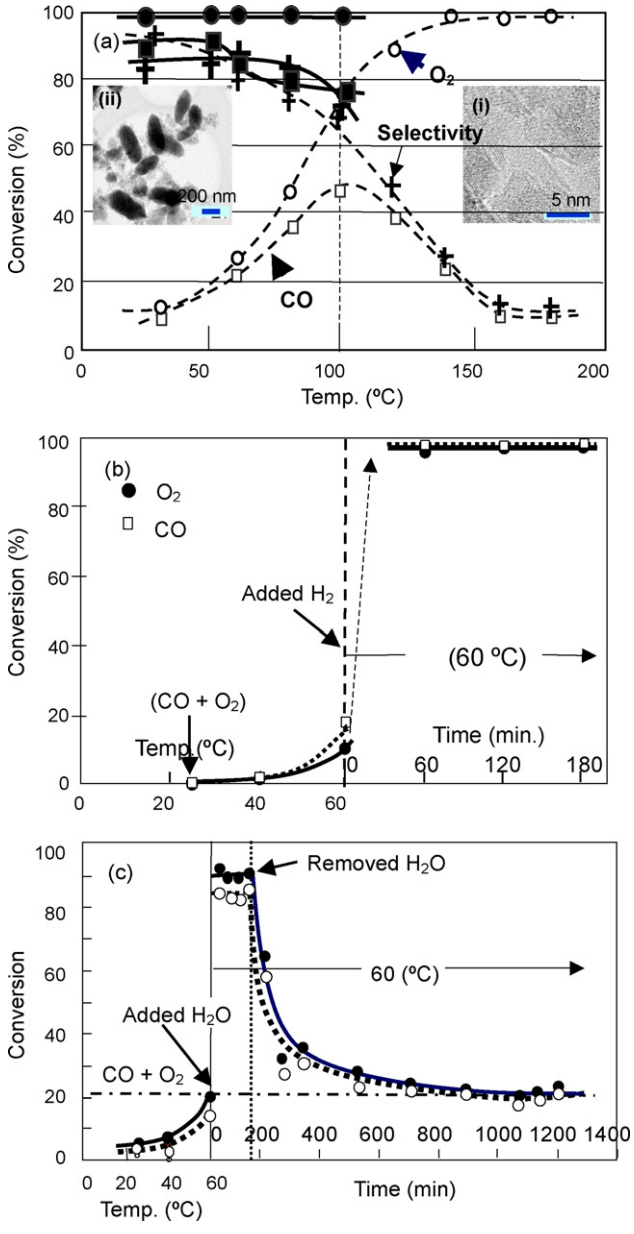

Fig. 6. (a) Conversion of CO and O_2 in a flowing a mixture of CO(3.0 ml/min) + O_2(1.5 ml/min) + H_2(20 ml/min) + N_2(75.5 ml/min) through 0.8 g of 1 wt.% Pt–TiO_2 catalyst (open symbols) and 0.8 g FeO_x/Pt/TiO_2 (0.4 wt.% Pt) catalyst (solid symbols). Inset TEM images are (i) Pt–TiO_2 and (ii) FeO_x/Pt/TiO_2. (b) Oxidation of CO enhanced by H_2 (20 ml/min) in a flow of CO(1.5 ml/min) + O_2(3 ml/min) + N_2(95.5 ml/min) at 60 °C. (c) Oxidation of CO enhanced by adding H_2O to the N_2 at 60 °C in a flow of CO(1.5 ml/min) + O_2(3 ml/min) + N_2(95.5 ml/mi) through a humidifier.

So far, a reaction mechanism of CO(a) + O(a) → CO_2 has been tacitly premised to explain the oxidation of CO, that is, no other specific mechanism was proposed even for the reaction at the perimeter of Au particles as well as on a (1×3) bi-layer structure of Au atoms. In this respect, Alayoglu et al. [55] published a notable paper to explain the specific activity of a Ru-core with Pt-shell catalyst.

They found specific activity of Pt-shell-layers on Ru-core (Pt-shell/Ru-core) nano-particles compared to the activity of Pt–Ru alloy particles and a mixture of Pt and Ru nano-particles for oxidation of CO in H_2 by a temperature programmed reaction in a flow of H_2 containing 1000 ppm ~1% CO and 0.5% O_2. The calculation was performed on several elementary reactions a Pt/Ru(0 0 0 1) as a model of Pt-shell/Ru-core particles and Pt(1 1 1). The binding energy and the activation barrier suggest that the oxidation of H_2 is facile on Pt/Ru(0 0 0 1) but the oxidation of CO with O_2 is facile on Pt(1 1 1), which are opposite to the observation on Pt particles and Pt-shell/Ru-core particles. To explain their experimental results, they proposed a hydrogen assisted dissociation of O_2 via hydroperoxy intermediate (HO_2), $H + O_2 \rightleftarrows HO_2 \rightarrow O + OH$, on Pt/Ru(0 0 0 1) by the calculation of activation barrier. From the calculation, they concluded that a H-assisted dissociation of O_2 was responsible for the preferential oxidation (PROX) reaction of CO in H_2 by Pt-shell/Ru-core catalyst. It should be pointed out that the competitive reaction of CO(a) + O(a) and H(a) + O(a) was tacitly assumed in their mechanism.

On the other hand, our proposed mechanism for the PROX reaction of CO in H_2 on the FeO_x/Pt–TiO_2 catalyst is entirely different. As shown in Fig. 6(b) and (c), the oxidation of CO is markedly enhanced by H_2 or H_2O on the FeO_x/Pt–TiO_2 catalyst but not on the Pt–TiO_2 catalyst [51]. Another notable feature is a hydrogen isotope effect of H_2/D_2 and H_2O/D_2O ($r_H > r_D$) on the oxidation of CO on the FeO_x/Pt–TiO_2 catalyst [56]. The isotope effect on the oxidation of CO cannot be rationalized by hydrogen assisted dissociation mechanism of O_2. To shed light on the catalysis, the intermediates and their dynamics should be studied in a flow of $(CO + O_2 + H_2)$ or $(CO + O_2)$ by in situ spectroscopy.

From this point of view, the dynamics of in situ DRIFT were studied in a flow of $CO + O_2$ and $CO + O_2 + H_2$ on Pt/TiO_2 and FeO_x/Pt/TiO_2 catalysts [57,58]. When CO in a flow of $(CO + O_2 + H_2)$ was stopped, reaction intermediates were removed according to the corresponding elementary steps. As shown in Fig. 7(a), decreasing of intermediates with time was obtained by subtracting a steady state spectrum in a flow of $(CO + O_2 + H_2)$ from time resolved in situ spectra. Very rapid growth of several negative peaks was observed at 60 °C by removing CO from a flow of $(CO + O_2 + H_2)$, which were gas phase CO (2119, 2172 cm^{-1}), adsorbed CO(a) (2069, 1836 cm^{-1}), HCOO(a) (1522, 1354, 1296 cm^{-1}), and OH(a) (broad band centered at 3350 cm^{-1}). In contrast, less rapid growing of the negative peaks assignable to CO(a) and bicarbonate (CO_2(OH)(a)) was observed by removing CO from a flow of $(CO + O_2)$ as shown in Fig. 7(b) and (c). These results proves that the oxidation of CO may proceed via different intermediates in $(CO + H_2 + O_2)$ and $(CO + O_2)$.

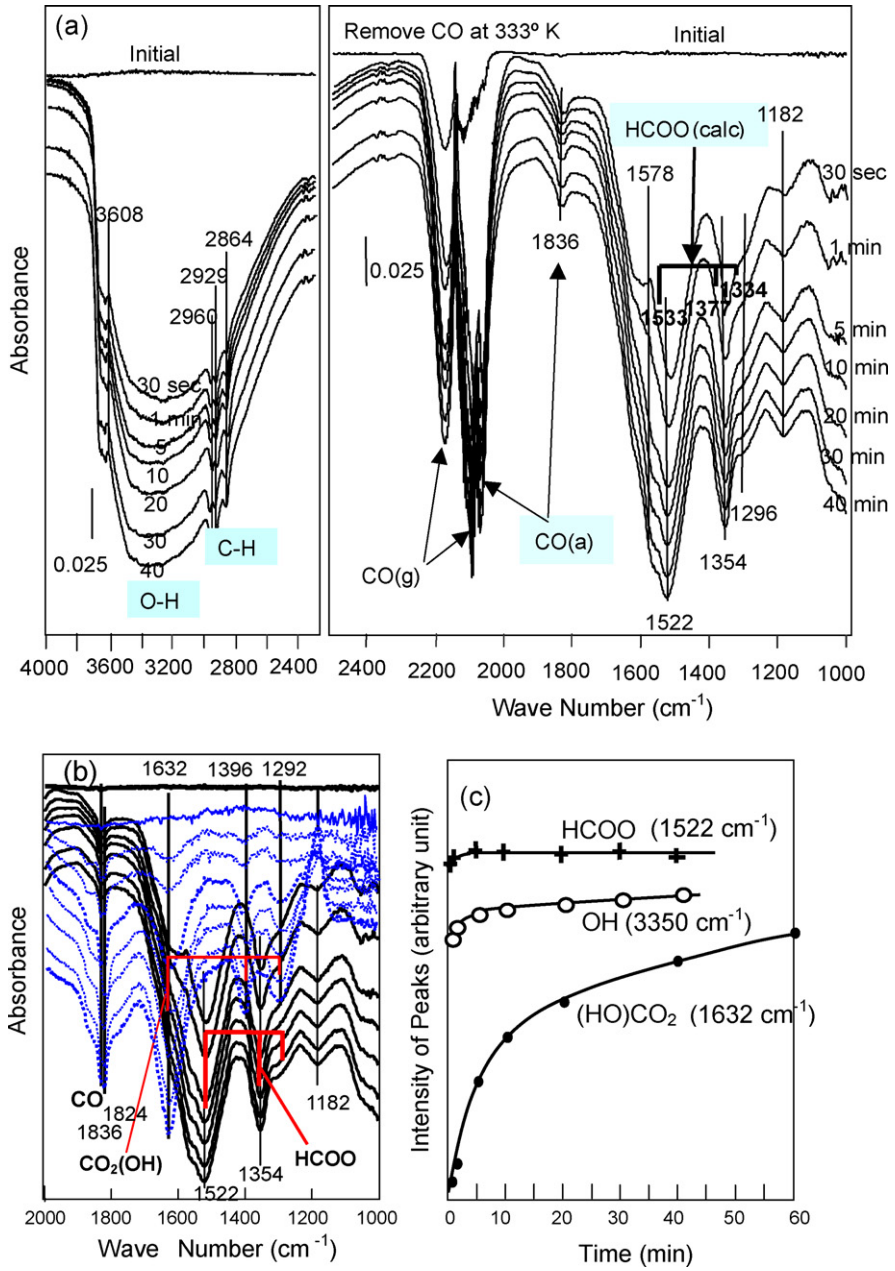

Fig. 7. (a) Dynamics of DRIFT spectra of FeO_x/Pt–TiO_2 catalyst attained by removing CO from a flow of ($CO + O_2 + H_2$) at 60 °C. Concomitant growth of the negative peaks of HCOO, OH (3000–3600 cm^{-1}), and C–H (2864, 2929, and 2960 cm^{-1}) indicates rapid reaction of HCOO with OH. (b) DRIFT spectra attained by removing CO from ($CO + O_2 + N_2$) and from ($CO + O_2 + H_2 + N_2$) on FeO_x/Pt–TiO_2 at 60 °C. (c) HCOO decreased very fast in H_2 but the decrease of bicarbonate CO_2(OH) was slow in the absence of H_2.

Another notable phenomenon is rapid growth of the negative broad OH(a) band relating to the negative growth of HCOO(a) peaks when CO is removed from a flow of ($CO + H_2 + O_2$) as shown in Fig. 7(a) [58]. It should be kept in mind that detectable intermediates by in situ DRIFT spectroscopy are the intermediates preceding the rate-determining step. In other word, the amount of intermediates after the rate-determining step is usually too low to detect. Taking these results into account, simultaneous rapid decrease of OH(a) and HCOO(a) reflects the rate-determining reaction of HCOO with OH in the PROX reaction of CO.

On the other hand, when H_2 in a flow of ($CO + O_2 + H_2$) was removed, the oxidation of CO was markedly suppressed although O_2 existed. The suppression was caused by decreasing of the OH species on Pt, that is, the reaction of HCOO with OH was disturbed. In fact, little change of CO(a) peak occurred by removing H_2 in a flow of ($CO + O_2 + H_2$), but rapid positive growth of HCOO(a) peaks was observed. This result is well explained by a dynamic balance of the formation and the reaction of HCOO intermediates, that is, provision of OH^- anion does not stop immediately because of slow decrease of adsorbed H_2O on the catalyst. Therefore, the formation of $HCOO^-$ intermediates is continued but the reaction of HCOO(a) with OH(a) on Pt, rate-determining step, becomes slow. As a result, the amount of HCOO(a) on the catalyst will increase for a time by removing H_2.

It should be reminded that the reaction of CO(a) with OH^- anion is a speculated reaction in our proposed mechanism. As we succeeded in developing an electro-conductive PROX catalyst being highly active at room temperature [58,59], we diagnosed the presence of OH^- anion on this PROX catalyst by combining with a polymer electrolyte hydrogen fuel cell (PEFC). If $HCOO^-$, precursor sate of HCOO intermediate, is provided by the reaction of CO(a) with OH^- anion, PROX reaction of CO will stop by contacting the catalyst

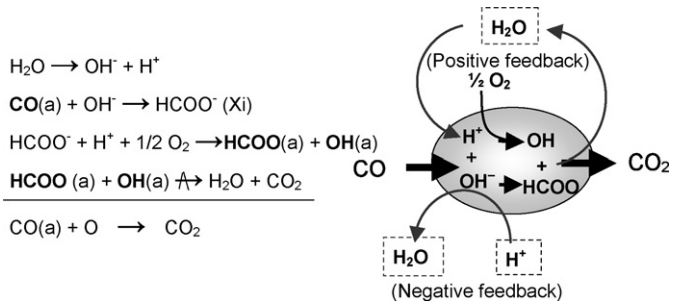

Scheme 4. Reaction of CO with OH^- anion is promoted by a positive feedback cycle given by H_2O, but the cycle stops by neutralization of OH^- with H^+.

with the anode of PEFC, because the OH^- anion is neutralized by H^+ ions diffusing from the anode side of the PEFC. In contrast, no suppression of the oxidation reaction of CO will occur when the inset catalyst is separated from the anode. Our prediction was perfectly supported by this new experiment. Accordingly, we conclude that the PROX reaction via HCOO intermediates is undoubtedly different from the reaction of CO(a) with O(a), and the reaction of HCOO(a) with OH(a) is responsible for the low temperature activity for the selective oxidation of CO in H_2. The hydrogen isotope effect on the oxidation of CO by H_2/D_2 and H_2O/D_2O is also well rationalized by this mechanism.

An over-all mechanism for the PROX reaction of CO on $FeO_x/Pt/TiO_2$ is described in Scheme 4, in which bold character indicates the intermediates observed by the DRIFT spectroscopy. As shown in this scheme, H_2O molecule plays an important role by enabling a positive feedback cycle by providing the OH^- anion on the $FeO_x/Pt–TiO_2$ catalyst. On the other hand, the reverse rotation is caused by H^+ which stops the PROX reaction of CO.

Finally, we wish to emphasize that the activity and/or selectivity improved by additives is not so simple as is explained by the activation barrier, the adsorption energy, and the characterization of catalyst without clarifying the reaction mechanism.

Acknowledgement

Author expresses his thanks to Mr. Mitsushi Umino of Astech Co. for his long time stimulation of my research works.

References

[1] I. Langmuir, Trans. Faraday Soc. 17 (1921) 607.
[2] L.H. Germer, Phys. Today 17 (719) (1964).
[3] G.C. Bond, Catalysis by Metals, Academic Press, London/NY, 1962.
[4] W.M.H. Sachtler, L.L.V. Reijen, Shokubai 4 (1962) 147 (in Japanese).
[5] K. Tanaka, K. Tamaru, J. Catal. 2 (1963) 366.
[6] H.S. Taylor, Proc. Roy. Soc. London, Ser. A108 (1925) 105.
[7] S.J. Thomson, J.L. Wishlade, Trans. Faraday Soc. 58 (1962) 1170.
[8] K. Tamaru, Adv. Catal. 15 (1964) 65;
K Tamaru, Bull. Chem. Soc. Jpn. 31 (1958) 666.
[9] S.L. Bernasek, W.L. Siekhaus, G.A. Somorjai, Phys. Rev. Lett. 30 (1973) 1202.
[10] S.M. Davis, F. Zaera, B.E. Gordon, G.A. Somorjai, J. Catal. 92 (1985) 240.
[11] D.R. Strongin, J. Carrazza, S.R. Bare, G.A. Somorjai, J. Catal. 103. (1987) 213.
[12] G. Binnig, H. Rohrer, C. Gerber, E. Weibel, Phys. Rev. Lett. 50 (1983) 120;
G. Binnig, H. Rohrer, Surf. Sci. 126 (1983) 236.
[13] G. Kleinle, Y. Penka, R.J. Behm, G. Ertl, Phys. Rev. Lett. 58 (1987) 148.
[14] T. Hashizume, M. Taniguchi, K. Motai, H. Lu, K. Tanaka, T. Sakurai, Jpn. J. Appl. Phys. 30 (1991) L1529.
[15] L.P. Nielsen, F. Besenbacher, E. Laesggaard, I. Stensgaard, Phys. Rev. B 44 (1991) 13156.
[16] P.T. Sprunger, Y. Okawa, F. Besenbacher, I. Stensgaard, K. Tanaka, Surf. Sci. 344 (1995) 98.
[17] K. Tanaka, Jpn. J. Appl. Phys. 32 (1993) 1389.
[18] K. Tanaka, Surf. Sci. 357–358 (1996) 721.
[19] Y. Matsumoto, K. Tanaka, Surf. Sci. 350 (1996) L227.
[20] K. Tanaka, Y. Okawa, Surf. Sci. 386 (1997) 56.
[21] F.C.M.J.M. van Delft, B.E. Nieuwenhuys, J. Siera, R.M. Wolf, ISIJ Int. 29 (1989) 550;
F.C.M.J.M. van Delft, B.E. Nieuwenhuys, J. Siera, R.M. Wolf, Surf. Sci. 264 (1992) 435.
[22] H. Hirano, T. Yamada, K. Tanaka, J. Siera, B.E. Nieuwenhuys, Surf. Sci. 222 (1989) L804;
H. Hirano, T. Yamada, K. Tanaka, J. Siera, B.E. Nieuwenhuys, Vacuum 41 (1990) 134.
[23] H. Tamura, A. Sasahara, K. Tanaka, J. Electroanal. Chem. 381 (1995) 95.
[24] H. Tamura, K. Tanaka, Langmuir 10 (1994) 4530.
[25] M. Taniguchi, E.K. Kuzembaev, K. Tanaka, Surf. Sci. 290 (1993) L711.
[26] H. Tamura, A. Sasahara, K. Tanaka, Surf. Sci. 303 (1994) L379.
[27] Y. Matsumoto, Y. Okawa, T. Fujita, K. Tanaka, Surf. Sci. 355 (1996) 109.
[28] K. Tanaka, Y. Okawa, A. Sasahara, Y. Matsumoto, in: A. Wieckowski (Ed.), Interfacial Electrochemistry, Marcel Dekker Inc., NY/Basel, 1999 (Chapter 18).
[29] S. Satokawa, J. Shibata, K. Shimizu, A. Satsuma, T. Hattori, Appl. Catal. B 42 (2003) 179.
[30] M. Richter, U. Bentrup, R. Eckelt, M. Schneide, M. Pohl, R. Fricke, Appl. Catal. B 51 (2004) 261.
[31] J. Shibata, Y. Takada, A. Satsuma, T. Hattori, S. Satokawa, J. Catal. 222 (2004) 368.
[32] J.P. Breen, R. Burch, C. Hardacre, C.J. Hill, J. Phys. Chem. B 109 (2005) 485.
[33] Y. Yu, H. He, Q. Feng, J. Phys. Chem. B 107 (2003) 13090.
[34] X. Zhang, Y. Yu, H. He, Appl. Catal. B.: Environ. 76 (2007) 241.
[35] Y. Yu, Q. Hong He, H. Feng, X. Gao, Yang, Appl. Catal. B 49 (2004) 159.
[36] C.A. Taatjes, N. Hansen, A. McIlroy, J.A. Miller, J.P. Senosiain, S.J. Klippenstein, F. Qi, L. Sheng, Y. Zhang, T.A. Cool, J. Wang, P.R. Westmoreland, M.E. Law, T. Kasper, K. Kohse-Höinghaus, Science 308 (2005) 1887.
[37] A. Kato, S. Matsuda, F. Nakajima, M. Imanari, Y. Watanabe, J. Phys. Chem. 85 (1981) 1710.
[38] R.B. Levy, M. Boudart, J. Catal. 32 (1974) 364.
[39] K. Tanaka, T. Okuhara, J. Catal. 78 (1982) 155.
[40] K. Tanaka, Advances in Catalysis, vol. 33, Academic Press, 1985, p. 99.
[41] K. Tanaka, T. Okuhara, S. Sato, K. Miyahara, J. Catal. 43 (1976) 360.
[42] K. Tanaka, Appl. Catal. A.: Gen. 188 (1999) 37.
[43] M. Kazuta, K. Tanaka, J. Chem. Soc., Chem. Commun. 616 (1987);
M. Kazuta, K. Tanaka, J. Catal. 123 (1990) 164.
[44] K. Tanaka, K. Tanaka, H. Takeo, C. Matsumura, J. Am. Chem. Soc. 109 (1987) 2422.
[45] M. Ikai, H. He, C.E. Borroni-Bird, H. Hirano, K. Tanaka, Surf. Sci. 315 (1994) L973.
[46] M. Ikai, K. Tanaka, Surf. Sci. 357–358 (1996) 781.
[47] M. Ikai, K. Tanaka, J. Phys. Chem. B 103 (1999) 8277.
[48] M. Ikai, K. Tanaka, J. Chem. Phys. 110 (1999) 7031.
[49] C. Hardacre, R.M. Ormerod, R.M. Lambert, J. Phys. Chem. 98 (1992) 10901.
[50] M. Shou, K. Tanaka, K. Yoshioka, Y. Moro-oka, S. Nagano, Catal. Today 90 (2004) 255.
[51] K. Tanaka, M. Shou, K. He, X. Shi, Catal. Lett. 110 (2006) 185.
[52] M. Shou, H. Takekawa, D.-Y. Ju, T. Hagiwara, K. Tanaka, Catal. Lett. 107 (2006) 119.
[53] M. Haruta, Catal. Today 36 (1997) 153.
[54] M.S. Chen, D.W. Goodman, Science 306 (2004) 252.
[55] S. Alayoglu, A.U. Nilekar, M. Mavrikakis, B. Eichhorn, Nat. Mater. 7 (2008) 333.
[56] M. Shou, K. Tanaka, Catal. Lett. 111 (2006) 115.
[57] X. Sie, K. Tanaka, H. He, M. Shou, W. Xu, X. Zhang, Catal. Lett. 120 (2008) 210.
[58] K. Tanaka, M. Shou, H. He, X. Sie, X. Zhang, J. Phys. Chem. C 113 (2009) 12427.
[59] K. Tanaka, M. Shou, H. He, C. Zhang, D. Lu, Catal. Lett. 127 (2009) 148.